Rare-earth-element ordering and structural variations in natural rare-earth-bearing apatites

John M. Hughes, Maryellen Cameron

Department of Geology, Miami University, Oxford, Ohio 45056, U.S.A.

Anthony N. Mariano

48 Page Brook Road, Carlisle, Massachusetts 01741, U.S.A.

Abstract

High-precision crystal structure refinements ($R < 0.02$) were undertaken on natural rare-earth-element-bearing apatites that contain 1.26, 0.85, 0.62, and 0.33 rare-earth atoms per ten Ca sites in the unit cell. Electron and ion microprobe analyses of the REE-substituted apatites indicate that charge balance for the altervalent $REE^{3+} \leftrightharpoons Ca^{2+}$ substitution is maintained by a combination of $REE^{3+} + Si^{4+} \leftrightharpoons Ca^{2+} + P^{5+}$ and $REE^{3+} + Na^{+} \leftrightharpoons 2Ca^{2+}$.

Variations in individual and mean interatomic distances reflect the cumulative effect of the following substitutions: $OH^{-} \leftrightharpoons F^{-}$ in the column anion sites, $Si^{4+} \leftrightharpoons P^{5+}$ in the tetrahedral sites, $REE^{3+} \leftrightharpoons Ca^{2+}$ in Ca sites, and $Na^{+} \leftrightharpoons Ca^{2+}$ in Ca sites. Mean Ca(1)-O distances in the crystals studied range from ~2.55 Å to ~2.57 Å and define regular, but not linear, increasing trends as a result of substitution of larger REE and Na atoms for Ca. Interatomic distances in the Ca(2) polyhedron are affected by both cation and anion substitutions, and thus variations are considerably less regular than those observed for Ca(1). Mean tetrahedral bond distances range from 1.536 Å to 1.542 Å and reflect the substitution of Si^{4+} for P^{5+}.

All four apatites studied are distinctly enriched in the light REEs. Structure refinements demonstrate that the light REEs (La → Sm), taken as a group, show a marked preference for the Ca(2) site in the apatite structure. Values of $REE_{Ca(2)}/REE_{Ca(1)}$, calculated per individual site to account for the different multiplicity of the two Ca sites, vary between 1.76 and 3.00 over the range of compositions studied. Bond valence calculations for substituent REEs in the apatite structures indicate that the preference of REEs for the Ca(2) site may be a function of differing preference of elements within the light REE group; these calculations suggest that La → Pr should preferentially substitute in the Ca(2) site, whereas Pm → Sm should selectively substitute at the Ca(1) site. The calculations also indicate that Nd^{3+} can readily substitute in either Ca site. These preferences can explain the variation in partition coefficients of the REE $^{3+}$ in apatite.

Introduction

Apatite minerals of composition $Ca_{10}(PO_4)_6(OH,F,Cl)_2$ are common accessory minerals in igneous, metamorphic, and sedimentary rocks. Although usually present only as an accessory phase in most igneous rocks, apatite plays a major role in the evolution of magmas; petrologists have shown that apatite is among the most important phases in controlling rare-earth-element variation in igneous rock (e.g., Nash, 1972; Bergman, 1979; Watson and Capobianco, 1981; Watson and Green, 1981; Kovalenko et al., 1982; Watson and Harrison, 1984a, 1984b).

Although numerous studies have been undertaken to elucidate the behavior of REEs in various geologic systems (e.g., Henderson, 1984; Lipin and McKay, 1989), few studies are available that investigate the behavior of those elements in the apatite structure, as determined on natural crystals. We present here high-precision crystal structure refinements of four natural apatites of varying REE composition in order to address the ordering of rare earth elements within the apatite structure and to elucidate the perturbations in the apatite atomic arrangement caused by substitution of REEs for Ca.

Previous work

The distribution of rare earth elements between the two Ca sites in apatite (depicted in Fig. 1) has been addressed in numerous studies in the last 25 years. Results of the studies are contradictory and indicate that REEs may partition preferentially into Ca(1) or Ca(2), or they may show no preference for either site. In a predictive study based on analysis of ligand type for each of the two Ca sites, Urasov and Khudolozhkin (1975) suggested that cations more electronegative than Ca will preferentially occupy the more covalent Ca(1) position, whereas those elements more electropositive than Ca will display a site preference for the more ionic Ca(2) position, thus over-
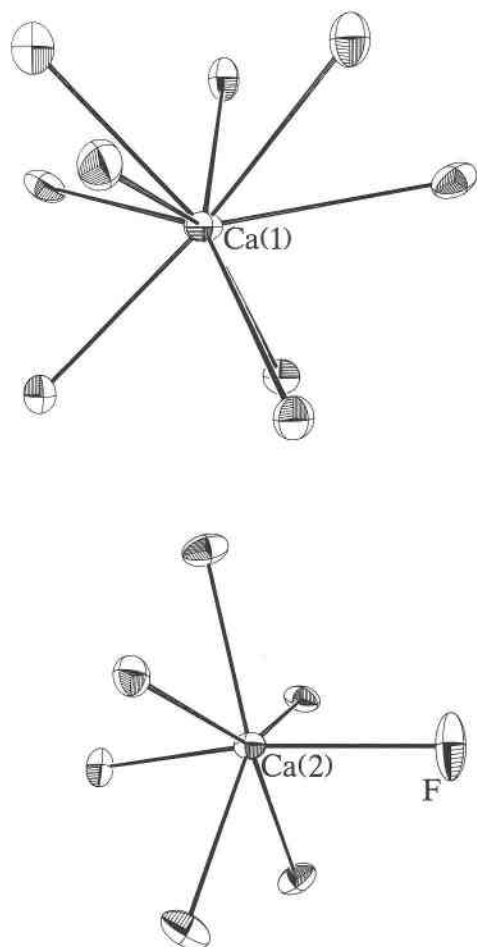
Fig. 1. Ca(1) and Ca(2) polyhedra in fluorapatite (Hughes et al., 1989). Oxygen atoms are not labeled.

TABLE 1. REE concentrations in analyzed apatites (ppm)

	Pajarito	Oka-B	Kipawa	Oka
La	38200	21200	16800	6574
	42200	33200	14200	8080
Ce	72600	36470	26400	12810
	71300	56400	28900	13700
Pr	7950	NA	2820	2102
	NA	NA	NA	NA
Nd	31600	12200	8230	4312
	25600	15600	8800	4160
Sm	4310	1450	1120	500
	2770	1680	1680	499
Eu	<510	310	NA	164
	137	308	167	103
Gd	2860	NA	NA	772
	1740	1030	1730	326
Tb	4144	68	NA	599
	NA	NA	NA	NA
Dy	<288	NA	697	26.1
	425	284	1540	131
Ho	<716	NA	NA	<96.0
	NA	NA	NA	NA
Er	<210.0	NA	875	<78.7
	74	91	859	46
Tm	<43.8	NA	NA	<70.0
	NA	NA	NA	NA
Yb	<149.3	37.5	176	<61.5
	36	61	557	27
Lu	<131.9	5.2	NA	<52.8
	NA	NA	NA	NA

Note: The first row of concentrations is from microprobe or NAA analyses of a crystal from an aliquot of the analyzed specimens; the second row is from ion probe analysis of the individual crystals used in the X-ray study (see Appendix 1).

Nd_2O_3 or NdF_3. For fluorapatite doped with Nd_2O_3, Nd was found to occupy the Ca(2) site exclusively, whereas for NdF_3-doped fluorapatite they found that the REE occupied the two Ca sites in approximately equal proportions. In their study, Mackie and Young inferred site occupancy from refined site multiplicity values using Ca scattering factors rather than modeling site occupancy using Ca and Nd scattering factors; they also assumed a model of $Nd^{3+} \rightarrow Ca^{2+}$ substitution without addressing the concomitant charge compensation.

riding site preferences based on radii considerations. Application of their predictive guidelines indicates that the light REEs, which have radii slightly larger than Ca and electronegativity values greater than Ca, should preferentially occupy the larger Ca(1) site.

In contrast to this predictive study, however, Borisov and Klevcova (1963) refined the structure of a REE-Sr-bearing apatite (0.32 REE atoms per unit cell) and concluded that the REEs replace Ca in the smaller Ca(2) polyhedron. The results of their study are not definitive, however; using film techniques, they refined the data to R values of 18 and 20% for $hk0$ and $h0l$ reflections, respectively. In an X-ray study of a synthetic La-bearing apatite, $Ca_4La_6(SiO_4)_6(OH)_2$, Cockbain and Smith (1967) concluded that the La atoms are randomly distributed between the two Ca sites, although their conclusion was based on the relative intensity of only four X-ray diffractions.

In a structure study of synthetic apatites doped with Nd, Mackie and Young (1973) concluded that the Nd site preference depended on whether the doping vehicle was

EXPERIMENTAL

The REE-bearing apatite specimens include samples from Pajarito, New Mexico (Roeder et al., 1987; labeled "Pajarito" in following text, tables, and figures), the Bond Zone of the Oka carbonatite (Mariano, 1985; labeled "Oka-B"), the Kipawa, Quebec nepheline syenite complex (labeled "Kipawa"), and a second sample from the Oka carbonatite (labeled "Oka"). The specimens analyzed in this study are all light REE enriched (Table 1; analytical details in Appendix 1); the LREEs (La → Sm) account for greater than 95% (atomic) of the total REE in the samples. Appendix 1 contains sample descriptions and chemical formulas for each sample.

Crystals from each aliquot were examined using precession methods to confirm hexagonal symmetry (Laue group $6/m$) and the absence of superstructure reflections. Unit-cell parameters were refined (no symmetry constraints) using diffraction angles from 25 automatically

TABLE 2. Crystal data and results of crystal structure refinements for REE-bearing apatites

	Pajarito	Oka-B	Kipawa	Oka
Size (mm)	$0.18 \times 0.12 \times 0.12$	$0.16 \times 0.16 \times 0.16$	$0.15 \times 0.15 \times 0.15$	$0.18 \times 0.16 \times 0.16$
Unit-cell dimensions				
Least squares a (Å)	9.406(3)	9.423(2)	9.3875(9)	9.401(2)
b (Å)	9.405(2)	9.418(1)	9.394(1)	9.399(1)
c (Å)	6.913(2)	6.916(1)	6.8988(9)	6.8941(9)
α (°)	90.02(2)	90.00(1)	89.99(1)	90.00(1)
β (°)	89.98(3)	90.01(1)	90.003(9)	89.99(2)
γ (°)	120.00(2)	120.00(1)	120.00(1)	120.02(2)
Structure refinement ($P6_3/m$) a (Å)	9.4052	9.4202	9.3908	9.3995
c (Å)	6.9125	6.9157	6.8988	6.8941
θ range	0–30°	0–30°	0–30°	0–30°
Reflections	$\pm h \pm k + l$	$\pm h + k + l$	$\pm h + k + l$	$\pm h + k + l$
Scan time	≤75 s	≤70 s	≤90 s	≤70 s
Scan type	$\theta/2\theta$	$\theta/2\theta$	$\theta/2\theta$	$\theta/2\theta$
Number of data	3309	1756	1740	1740
Unique data	557	562	557	557
R_{merge}	0.019	0.017	0.018	0.016
Reflections $I > 3\sigma_I$	419	446	415	455
Refined parameters	42	43	42	42
R	0.015	0.019	0.018	0.017
R_w	0.018	0.029	0.025	0.026
$\Delta\rho$ residua (e Å⁻³) (+)	0.298	0.590	0.339	0.392
(−)	0.372	0.411	0.314	0.377

Note: For Table 2 and subsequent tables, numbers in parentheses denote 1 esd of the least significant digit.

centered diffractions measured on an Enraf-Nonius CAD4 single-crystal diffractometer. Intensity data were measured on the same instrument, and either three (Oka-B, Kipawa, Oka) or six (Pajarito) symmetry equivalents were obtained for each reflection. Absorption was corrected using an empirical ψ-scan technique employing intensity data obtained from 360° ψ scans collected at 10° intervals. Details of data collection and structure refinement are contained in Table 2.

Crystal structure calculations were undertaken in space group $P6_3/m$ using the SDP set of programs (Frenz, 1985). Neutral-atom scattering factors were employed, including terms for anomalous dispersion. Reflections with $I < 3\sigma_I$ were considered unobserved, and observed reflections were weighted proportional to σ_I^{-2}, with a term to de-emphasize intense reflections. Full-matrix least-squares refinement was undertaken by refining positional parameters, scale factor, anisotropic temperature factors, an isotropic extinction factor, and site occupancy for the Ca(1) and Ca(2) sites. The column anions were modeled using only F for the Pajarito and Kipawa samples, in accord with the microprobe analyses. For the Oka-B and Oka samples, both F and O(H) were included as column anions, as significant OH (obtained by difference) was indicated by the chemical analyses. For Oka-B the F temperature factors were fixed at those of F in the fluorapatite of Hughes et al. (1989); for the Oka sample, the small amount of OH necessitated fixing the O(H) position and thermal parameters at those of O(H) in the hydroxylapatite of Hughes et al. (1989).

Although Na has been found to occupy both Ca sites in studies of apatite structures, Na was assigned exclusively to the Ca(1) site in our refinements in order to provide a limiting case for REE ordering. Because there is a positive correlation between REE occupancy and Na

occupancy resulting from the differing scattering power of these elements relative to Ca, the observed site preference of the REEs for Ca(2) thus represents a minimum, i.e., any Na actually present in the Ca(2) site requires additional REE occupancy to yield the observed scattering power.

Rare earth atoms were modeled with Ce scattering factors, as Ce ($Z = 58$) is the most abundant REE in each apatite. The weighted average of $Z_{REE} = 58.2, 58.1, 58.7,$ and 58.0 for the Pajarito, Oka-B, Kipawa, and Oka samples, respectively. Ca and "Ce" occupancy was refined for each Ca site; because of the inherent difficulties in analyzing rare earth elements, particularly by electron microprobe, we did not constrain "Ce" occupancy to match the chemical analysis as we are more confident in occupancies obtained from the refinement of our high-precision X-ray diffraction data. For the Pajarito material, "Ce" content refined to 1.26 atoms per unit cell vs. 1.21 (Y + REE) from the ion probe analysis of the same crystal. For the Oka-B material, "Ce" content refined to 0.85 atoms per unit cell; the ion probe analysis of the same crystal yielded 0.84 (Y + REE) atoms. For the Kipawa apatite, "Ce" content refined to 0.62 atoms per unit cell vs. 0.51 (Y + REE) atoms by ion probe. The Oka material yielded 0.33 "Ce" atoms per unit cell by structure refinement and 0.20 (Y + REE) atoms by ion probe analysis of the same crystal.

Table 3 contains positional parameters and isotropic temperature factors for atoms in the four structures, and Table 4[1] presents anisotropic temperature factors. Table

---

[1] A copy of Tables 4 and 7 may be ordered as Document AM-91-461 from the Business Office, Mineralogical Society of America, 1130 Seventeenth Street NW, Suite 330, Washington, DC 20036, U.S.A. Please remit $5.00 in advance for the microfiche.

TABLE 3. Positional parameters and equivalent isotropic temperature factors (Å²) for REE-bearing apatite

	x	y	z	B
Ca(1)				
Pajarito	⅔	⅓	−0.0012(1)	0.986(7)
Oka-B	⅔	⅓	0.0004(1)	1.101(9)
Kipawa	⅔	⅓	0.0007(1)	1.023(9)
Oka	⅔	⅓	0.0011(1)	0.893(8)
Ca(2)				
Pajarito	−0.01140(4)	0.23885(4)	¼	0.885(6)
Oka-B	−0.00912(6)	0.24301(6)	¼	1.000(9)
Kipawa	−0.00867(6)	0.24026(6)	¼	1.018(9)
Oka	−0.00788(5)	0.24276(5)	¼	0.842(8)
P				
Pajarito	0.36881(7)	0.39692(7)	¼	0.63(1)
Oka-B	0.36896(9)	0.39824(9)	¼	0.73(1)
Kipawa	0.36928(8)	0.39832(8)	¼	0.72(1)
Oka	0.36875(7)	0.39813(7)	¼	0.57(1)
O(1)				
Pajarito	0.4821(2)	0.3233(2)	¼	1.14(3)
Oka-B	0.4842(2)	0.3261(3)	¼	1.08(4)
Kipawa	0.4843(2)	0.3261(2)	¼	1.09(4)
Oka	0.4849(2)	0.3269(2)	¼	0.96(3)
O(2)				
Pajarito	0.4671(2)	0.5853(2)	¼	1.35(4)
Oka-B	0.4659(3)	0.5874(3)	¼	1.35(5)
Kipawa	0.4667(3)	0.5875(2)	¼	1.23(5)
Oka	0.4659(2)	0.5873(2)	¼	1.08(4)
O(3)				
Pajarito	0.2557(1)	0.3396(2)	0.0721(2)	1.65(3)
Oka-B	0.2567(2)	0.3421(2)	0.0708(3)	1.72(3)
Kipawa	0.2572(2)	0.3417(2)	0.0704(3)	1.47(3)
Oka	0.2573(1)	0.3421(2)	0.0705(2)	1.32(2)
F				
Pajarito	0	0	¼	2.50(6)
Oka-B	0	0	¼	1.9
Kipawa	0	0	¼	2.56(7)
Oka	0	0	¼	2.7(1)
O(H)				
Pajarito	—	—	—	—
Oka-B	0	0	0.304(2)	2.3(2)
Kipawa	—	—	—	—
Oka	0	0	0.302	1.3

TABLE 5. Selected bond lengths for REE-bearing apatites

	Pajarito	Oka-B	Kipawa	Oka
Ca(1)-O(1) (×3):	2.424(1)	2.413(2)	2.404(2)	2.400(2)
O(2) (×3):	2.467(2)	2.459(2)	2.458(2)	2.457(2)
O(3) (×3):	2.827(2)	2.811(2)	2.807(2)	2.807(2)
Mean	2.573	2.561	2.556	2.555
Ca(2)-O(1):	2.639(1)	2.677(2)	2.680(2)	2.691(2)
O(2):	2.401(2)	2.379(2)	2.388(2)	2.376(2)
O(3) (×2):	2.357(2)	2.356(2)	2.352(2)	2.350(2)
O(3) (×2):	2.518(1)	2.518(2)	2.509(2)	2.508(1)
F:	2.3019(4)	2.3334(6)	2.2981(6)	2.3197(6)
OH:	—	2.363(2)	—	2.3473(5)
Mean$_{oxy}$	2.465	2.467	2.465	2.464
P-O(1):	1.534(2)	1.542(3)	1.536(3)	1.540(2)
O(2):	1.535(2)	1.543(2)	1.539(2)	1.540(2)
O(3) (×2):	1.537(1)	1.541(2)	1.538(2)	1.534(2)
Mean	1.536	1.542	1.538	1.537

Note: For all four structures Na was constrained to occupy Ca(1) exclusively.

5 contains selected bond distances, and Table 6 gives occupancies of the Ca sites in the apatite structures. Table 7 gives observed and calculated structure factors.

RARE EARTH ELEMENTS IN THE APATITE STRUCTURE

Cation polyhedra

In the apatite structure, two symmetrically distinct Ca polyhedra (Fig. 1) are hexagonally disposed about a central [001] hexad and are linked through O atoms shared with phosphate tetrahedra. The occupant of the larger Ca(1) site (point symmetry 3; multiplicity = 4) bonds to nine O atoms [3 × O(1), 3 × O(2), 3 × O(3)], whereas the occupant of the Ca(2) site (point symmetry *m*; multiplicity 6) bonds to six O atoms and one column anion. Column anions, F and OH in this study, lie on the [001] hexads.

Variations in individual and mean interatomic distances (Table 5 and Figs. 2–4) in cation polyhedra of the REE apatites reflect the cumulative effect of four substitutions: OH⁻ ⇌ F⁻ in the column anion sites, Si^{4+} ⇌ P^{5+} in the tetrahedral sites, REE^{3+} ⇌ Ca^{2+} in Ca sites, and Na^+ ⇌ Ca^{2+} in Ca sites. Mean Ca(1)-O distances (Fig. 2) range from ~2.55 to ~2.57 Å for the REE samples of this study, compared to ~2.55 Å for fluorapatite and hydroxylapatite examined by Hughes et al. (1989). Ca(1)-O distances (Fig. 2) for the Oka, Kipawa, and Oka-B samples generally show slight but regular increases with increasing REE content. The increases are consistent with substitution of larger LREE or Na atoms for Ca. The Pajarito bond distances are significantly longer than expected by linear extrapolation of trends defined for other samples, probably a result of significant Na substitution (0.95 atom per unit cell).

Ca(2)-O distances (Fig. 3) are affected by both cation and anion substitutions, and thus variations at Ca(2) among the four REE apatites are considerably less regular than those observed for the Ca(1) polyhedron. Individual Ca(2)-O(1) bond lengths define a regular decreasing trend, whereas individual Ca(2)-O(3) bond lengths define a regular increasing trend with increasing REE content of the site. Individual Ca(2)-O(2) and Ca(2)-O(3)′ distances exhibit irregular variations presumably because of effects from substitutions involving the OH-F column anions.

TABLE 6. Site occupancies and Na, Si contents for REE apatites

	Total REEs*	REE/site	REE$_{Ca(2)}$/REE$_{Ca(1)}$	Na**	Si**
Pajarito					
Ca(1)	0.346(3)	0.087	1.76	0.95	0.32
Ca(2)	0.915(4)	0.153			
Total	1.261				
Oka-B					
Ca(1)	0.205(4)	0.051	2.10	0.04	0.81
Ca(2)	0.642(5)	0.107			
Total	0.847				
Kipawa					
Ca(1)	0.154(4)	0.039	1.97	0.10	0.44
Ca(2)	0.463(5)	0.077			
Total	0.617				
Oka					
Ca(1)	0.060(3)	0.015	3.00	0.02	0.32
Ca(2)	0.267(4)	0.045			
Total	0.327				

Note: Values for total REEs and Na, Si in atoms per unit cell.
* Obtained from structure refinements.
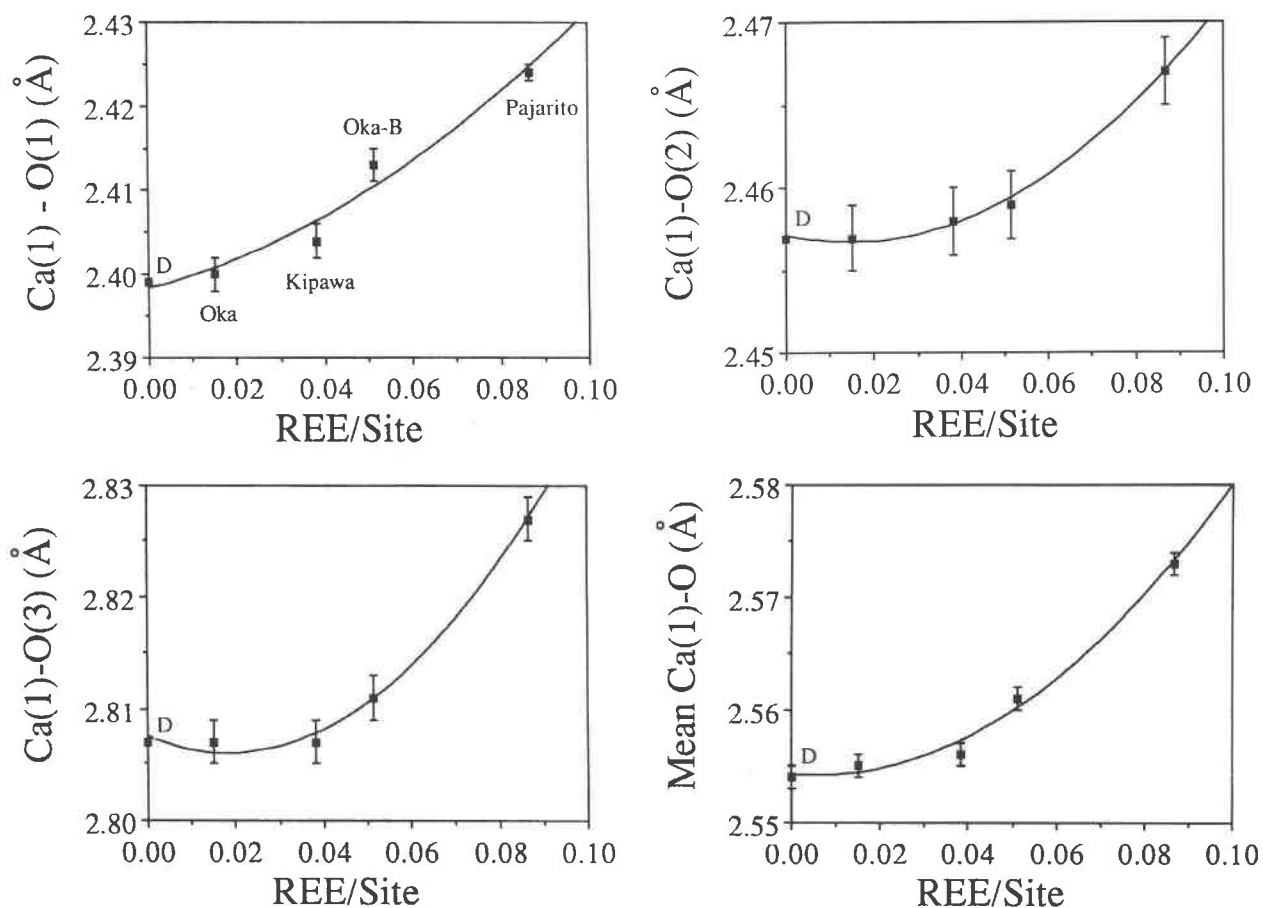** Obtained from microprobe analysis.

Fig. 2.   Variation of bond lengths in Ca(1) polyhedron with refined REE/site for each crystal. Error bars represent ±1 esd. Curves show second-order fits to all five data points. Points labeled "D" are from Durango fluorapatite of Hughes et al. (1989).

Normalization of Oka and Oka-B samples, both of which contain significant OH, to a fluorapatite end-member produces a smooth curve that contains all data points (see insets in Fig. 3). Mean Ca(2)-O = ~2.46 Å for the REE apatites of this study and for the fluorapatite and hydroxylapatite of Hughes et al. (1989).

Variations in mean tetrahedral distances (Fig. 4) for the four REE apatites of this study reflect the substitution of Si^{4+} for P^{5+}. Mean distances range from 1.536 Å to 1.542 Å, in comparison to 1.537 Å and 1.534 Å for fluorapatite and hydroxylapatite, respectively (Hughes et al., 1989).

Site occupancy

Table 6 presents the occupancies of the Ca(1) and Ca(2) sites for the four apatite structures as obtained from the structure refinements. These distributions indicate that the rare earth elements are not excluded from either Ca site, but they display a distinct site preference for the Ca(2) site in the phosphate apatite atomic arrangement. The ratios of $REE_{Ca(2)}/REE_{Ca(1)}$ in the four crystals studied vary between 1.76 and 3.00 [the ratios are calculated per individual site, accounting for the different multiplicity of the Ca(1) and Ca(2) sites].

Ionic radii for the REEs from La → Lu range from ~1.10 Å to 0.92 Å for sevenfold coordination and from ~1.22 Å to 1.03 Å for ninefold coordination. The sevenfold ligation approximates that for the apatite Ca(2) site, whereas the ninefold coordination approximates the configuration for the apatite Ca(1) site. In detail, the radius of the $^{[9]}Ca^{2+}$ (1.18 Å) in Ca(1) is most similar to that of the lightest REEs (for example, $^{[9]}Ce^{3+}$ = 1.196 Å), and the radius of $^{[7]}Ca^{2+}$ (1.06 Å) in Ca(2) is also most similar to the lightest REEs (e.g., $^{[7]}Ce^{3+}$ = 1.07 Å) (radii values from Shannon, 1976).

In addition to radius constraints, bond valence requirements must be met in the substitution of the REEs for Ca. The suitability of any REE for either Ca site was estimated on the basis of its bond valence sum. Table 8 gives the bond valence sums for all REEs in the Ca sites of the analyzed apatites with the valence of the preferred site for substituent REEs underlined for values within an arbitrary 10% of the formal valence (3^+). The cause of the selective concentration of the light REEs in the analyzed apatite structures is immediately evident in that table; the REEs from Gd → Lu are severely underbonded in either Ca site. Differences in site preference among the
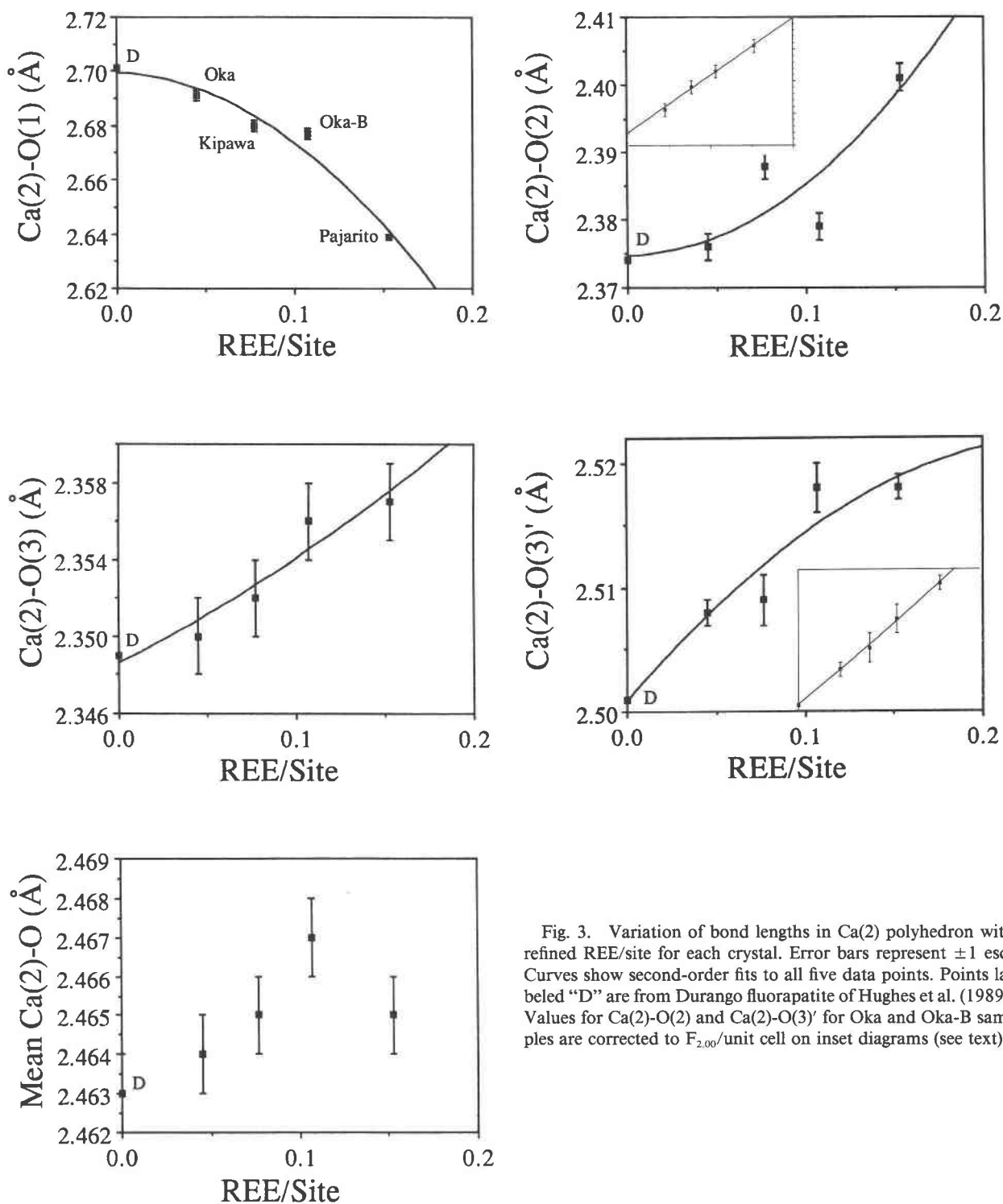
Fig. 3. Variation of bond lengths in Ca(2) polyhedron with refined REE/site for each crystal. Error bars represent ±1 esd. Curves show second-order fits to all five data points. Points labeled "D" are from Durango fluorapatite of Hughes et al. (1989). Values for Ca(2)-O(2) and Ca(2)-O(3)' for Oka and Oka-B samples are corrected to $F_{2.00}$/unit cell on inset diagrams (see text).

light REEs are also evident. The bond valence sums indicate a preference for the Ca(2) site for La, Ce, and Pr, as these REEs would be even more overbonded if they were to occupy the Ca(1) site. Conversely, this analysis suggests that Pm and Sm should prefer the Ca(1) site, as they would be more underbonded in the Ca(2) site compared to Ca(1). The bond sums for Nd in the analyzed apatites show that it should readily substitute on both
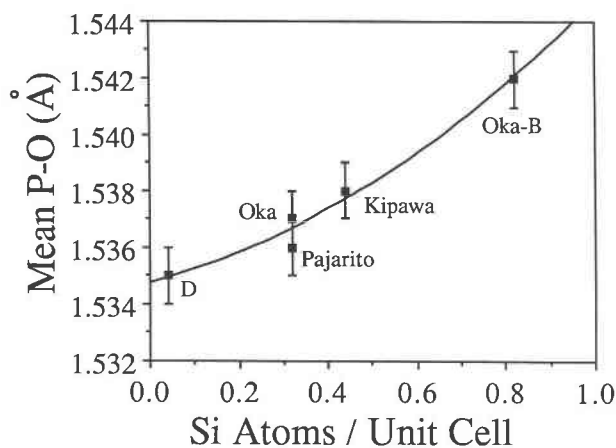
Fig. 4. Variation of bond lengths in phosphate tetrahedra with total Si content of each crystal. Error bars represent ±1 esd. Curves show second-order fits to all five data points. Point labeled "D" is from Durango fluorapatite of Hughes et al. (1989).

TABLE 8. Bond-valence sums for REE^{3+} in Ca(1) and Ca(2) sites of refined apatite structures

	Pajarito	Oka-B	Kipawa	Oka
La*				
Ca(1)	3.27	3.36	3.41	3.43
Ca(2)	3.20	3.25	3.23	3.26
Ce				
Ca(1)	3.20	3.29	3.34	3.36
Ca(2)	3.12	3.17	3.15	3.18
Pr				
Ca(1)	3.11	3.20	3.24	3.26
Ca(2)	3.03	3.08	3.05	3.08
Nd				
Ca(1)	2.99	3.07	3.11	3.13
Ca(2)	2.91	2.96	2.94	2.96
Pm				
Ca(1)	2.84	2.92	2.96	2.97
Ca(2)	2.77	2.81	2.80	2.82
Sm				
Ca(1)	2.73	2.80	2.84	2.86
Ca(2)	2.66	2.70	2.69	2.71
Eu				
Ca(1)	2.59	2.66	2.69	2.71
Ca(2)	2.53	2.57	2.56	2.58
Gd				
Ca(1)	2.48	2.55	2.59	2.60
Ca(2)	2.43	2.46	2.46	2.47
Tb				
Ca(1)	2.39	2.46	2.49	2.51
Ca(2)	2.34	2.37	2.37	2.38
Dy				
Ca(1)	2.30	2.37	2.40	2.41
Ca(2)	2.26	2.29	2.28	2.30
Ho				
Ca(1)	2.22	2.28	2.31	2.32
Ca(2)	2.18	2.20	2.20	2.21
Er				
Ca(1)	2.13	2.19	2.22	2.24
Ca(2)	2.10	2.12	2.12	2.13
Tm				
Ca(1)	2.07	2.13	2.16	2.17
Ca(2)	2.04	2.06	2.06	2.07
Yb				
Ca(1)	2.02	2.08	2.10	2.12
Ca(2)	1.99	2.01	2.01	2.02
Lu				
Ca(1)	1.97	2.02	2.05	2.06
Ca(2)	1.94	1.96	1.96	1.97

* Bond-valence sums were calculated from constants of Brown (1981). The value of the preferred site for substituent REEs, as suggested by the bond-valence sum, is underlined for values within 10% of the formal valence.

sites. Thus, this generalized bond valence analysis suggests that the light REEs may not behave as a chemically coherent group during substitution in the apatite structure. It also indicates that distribution coefficients of REE^{3+} in apatite should display a generally concave downward pattern centered on Nd^{3+}, with somewhat higher partition coefficients for the LREE compared to the HREE. These variations can be explained in terms of the Ca sites available to the various REEs. For example, Nd will have ten preferred sites in the apatite structure, in contrast to the lighter REEs, which will have six preferred sites [the $6h$ Ca(2) sites], and heavier REEs, which will have four preferred sites [the $4f$ Ca(1) sites]. This pattern of concave downward REE distributions has been found in petrologic studies of apatites in natural and synthetic systems (e.g., Nagasawa, 1970; Watson and Green, 1981).

Although REEs in all four samples studied exhibit a distinct preference for the Ca(2) site, significant differences exist in the ratio of $REE_{Ca(2)}/REE_{Ca(1)}$ among the samples (Table 6). The observed site preference of the light REEs, taken as a group, for the Ca(2) site may largely be a function of a site preference of La + Ce for the Ca(2) site, those elements being the most abundant REEs in the analyzed specimens.

Charge balance

The substitution of REE^{3+} for Ca^{2+} in the apatite structure requires a concomitant altervalent substitution to maintain charge balance. In an investigation of the chemistry of REE-bearing apatites in alkaline rocks from the Ilimaussaq intrusion, Ronsbo (1989) showed that charge balance in those apatites is maintained by the substitutions $REE^{3+} + Si^{4+} \rightleftharpoons Ca^{2+} + P^{5+}$ or $REE^{3+} + Na \rightleftharpoons 2Ca^{2+}$. In the apatites from various rocks from the intrusion, the particular charge-balance mechanism employed was found to be a function of magma chemistry.

Table 6 gives the Na and Si content of the apatites studied herein, and Figure 5 is a plot of atomic (Na + Si) vs. refined REE. The correlation of the variables and the near-zero intercept demonstrate that in these apatites charge balance is maintained by a combination of the above substitutions (Na $\rightleftharpoons$ Ca, Si $\rightleftharpoons$ P) and not by other mechanisms such as vacancies in the structure. The apatites studied differ in the particular charge balance mechanism employed. The atomic ratio of substituent Na:Si varies from 2.97 (Pajarito) to 0.05 (Oka-B). For either substitution local charge balance is maintained by
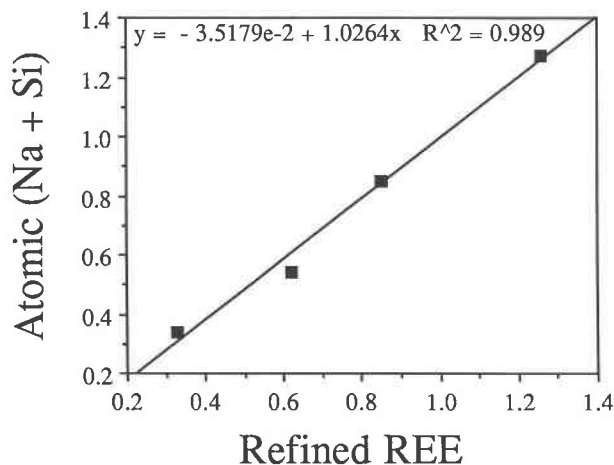
Fig. 5. Atomic (Na + Si) vs. refined REE, per unit cell.

the presence of the REE in an adjacent polyhedron. Thus, the REE substituent would be linked through a bridging O atom to Si in an adjacent phosphate tetrahedron or Na in an adjacent Ca(1) or Ca(2) site.

SUMMARY

The importance of REEs in petrologic studies has increased to the point where rare earth variation patterns are an almost essential component of most studies addressing petrogenesis of igneous rocks. It is not clear, however, that the behavior of REEs within and among minerals is understood well enough to provide a foundation for understanding their behavior in rocks. In a crystalline rock, each REE must have a mineralogical site in which to reside, and the REE variation in rocks is merely a function of the available mineral sites for substituent REEs.

The results of this study suggest that the rare earth group of elements can no longer be viewed as having two members, LREE and HREE. It appears that the cation sites in common minerals such as apatite effectively discriminate among members of these groups in petrologic processes in a manner that is predictable with knowledge of their atomic arrangements. We are now undertaking high-precision crystal structure studies of REE-bearing minerals in order to characterize those sites that accommodate the REEs and elucidate their response to different concentrations of substituent REEs.

REFERENCES CITED

Bergman, S.C. (1979) The significance of accessory apatite in the REE modelling of magma genesis. Eos, 60, 412.

Borisov, S.V., and Klevcova, R.F. (1963) The crystal structure of RE-Sr apatite. Zhurnal Strukturnoi Khimii, 4, 629–631 (not seen; abstracted from Structure Reports, 28, 188–189, 1963).

Brown, I.D. (1981) The bond-valence method: An empirical approach to chemical structure and bonding. In M. O'Keeffe and A. Navrotsky, Eds., Structure and bonding in crystals II, p. 1–30. Academic Press, New York.

Cockbain, A.G., and Smith, G.V. (1967) Alkaline-rare-earth silicate and germanate apatites. Mineralogical Magazine, 36, 411–421.

Eby, G.N. (1975) Abundance and distribution of the rare earth elements and yttrium in the rocks and minerals of the Oka carbonatite complex, Quebec. Geochimica et Cosmochimica Acta, 39, 597–620.

Frenz, B.A. (1985) Enraf-Nonius structure determination package. SDP users guide, version 4. Enraf-Nonius, Delft, The Netherlands.

Henderson, P. (1984) Rare earth element geochemistry, 510 p. Elsevier, The Netherlands.

Hughes, J.M., Cameron, M., and Crowley, K.D. (1989) Structural variations in natural F, OH, and Cl apatites. American Mineralogist, 74, 870–876.

Kovalenko, V.I., Antipin, V.S., Vladykin, N.V., Smirnova, Ye.V., and Balashov, Yu.A. (1982) Rare-earth distribution coefficients in apatite and behavior in magmatic processes. Geokhimiya, 2, 230–243.

Lipin, B.R., and McKay, G.A. (1989) Geochemistry and mineralogy of rare earth elements. In Mineralogical Society of America Reviews in Mineralogy, vol. 21.

Mackie, P.E., and Young, R.A. (1973) Location of Nd dopant in fluorapatite, $Ca_5(PO_4)_3F:Nd$. Journal of Applied Crystallography, 6, 26–31.

Mariano, A.N. (1984) Preliminary characterization of mineralogy and cathodoluminescence on some alkaline rocks from Pajarito Mountain, New Mexico. Confidential report to Molycorp, Inc., Louviers, Colorado.

Mariano, C.G. (1985) The paragenesis of the bond zone of the Oka carbonatite complex, Oka, Quebec, 57 p. Unpublished senior thesis, Bucknell University, Lewisburg, Pennsylvania.

Nagasawa, H. (1970) Rare earth concentrations in zircons and apatites and their host dacites and granites. Earth and Planetary Science Letters, 9, 359–364.

Nash, W.P. (1972) Apatite chemistry and phosphorus fugacity in a differentiated igneous intrusion. American Mineralogist, 57, 877–886.

Roeder, P.L., MacArthur, D., Ma, X.-P., Palmer, G.R., and Mariano, A.N. (1987) Cathodoluminescence and microprobe study of rare-earth elements in apatite. American Mineralogist, 72, 801–811.

Ronsbo, J.G. (1989) Coupled substitutions involving REEs and Na and Si in apatites in alkaline rocks from the Ilimaussaq intrusion, South Greenland, and the petrological implications. American Mineralogist, 74, 896–901.

Shannon, R.D. (1976) Revised effective ionic radii and systematic studies of interatomic distances in halides and chalcogenides. Acta Crystallographica, A32, 751–767.

Urasov, V.S., and Khudolozhkin, V.O. (1975) An energy analysis of cation ordering in apatite. Geochemistry International, 11, 1048–1053.

Watson, E.B., and Capobianco, C.J. (1981) Phosphorus and the rare-earth elements in felsic magmas: An assessment of the role of apatite. Geochimica et Cosmochimica Acta, 45, 2349–2358.

Watson, E.B., and Green, T.H. (1981) Apatite/liquid partition coefficients for the rare earth elements and strontium. Earth and Planetary Science Letters, 56, 405–421.

Watson, E.B., and Harrison, T.M. (1984a) Accessory minerals and the geochemical evolution of crustal magmatic systems: A summary and prospectus of experimental approaches. Physics of the Earth and Planetary Interiors, 35, 19–30.

——— (1984b) What can accessory minerals tell us about felsic magma evolution? A framework for experimental study. Proceedings of the 27th International Geologic Congress, 11, 503–520.

APPENDIX 1. SAMPLE DESCRIPTIONS AND ANALYTICAL METHODS

Major element analyses of the crystals used in this study were obtained by electron microprobe from the laboratories listed below. Major and rare earth concentrations for aliquots of the Pajarito and Oka apatite samples, as obtained by electron microprobe, are reported in Roeder et al. (1987); the major element and REE analyses of an aliquot of the Kipawa sample were also obtained from microprobe analysis in that same laboratory (P. Roeder, personal communication). REE analysis of the Oka-B sample was obtained from NAA analysis of an aliquot of the Oka-B sample (Mariano, 1985), and major elements were analyzed at the Southern Methodist University microprobe facility. The REE concentrations listed in the first row in Table 1 for each element were obtained as described above.

The individual crystals used in the X-ray refinements were also analyzed for REE concentrations. The analyses were performed on a Cameca IMS 3f ion microprobe at Surface Science Western at the University of Western Ontario (Neil D. MacRae, analyst). Because the REE concentrations of the analyzed samples lie outside the range of the standards for many REE, the results are considered semiquantitative. Standards used were Durango apatite and apatite from Snarum, Norway (Roeder et al., 1987). Calibration curves were also constrained to pass through the zero intensity, zero concentration points (MacRae, personal communication). REE concentrations in the second row of Table 1 are from the ion probe analyses of the individual crystals used in the X-ray portion of the study. The formulas given below for the crystals are calculated from the microprobe data listed above (major elements) and the ion probe data (REE).

Pajarito. Sample T-654-0 of Roeder et al. (1987) from Pajarito Mountain, Otero County, New Mexico. The apatite is an accessory mineral in a Proterozoic peralkaline riebeckite granite and quartz syenite; other accessory phases include elpidite, zircon, thorite, gittinsite, and allanite. The bulk rock REE distribution at Pajarito is considerably more MREE enriched than the apatite. The LREE dominance of the Pajarito apatite is attributed to the early crystallization of apatite coupled with the relatively lower solubility of the LREE as opposed to the HREE and also

to the strong affinity of REE for phosphate. Late crystallization of kainosite veins (Mariano, 1984) and secondary zircon, both containing appreciable Y and HREE, attest to the buildup of HREE in the residual fluids. The REE distribution in Pajarito apatite cannot be used in this case as an indication of the bulk rock geochemistry. The Pajarito apatite analysis yields $(Ca_{7.67}Na_{0.95}Mn_{0.01}Fe_{0.03}Sr_{0.02}Y_{0.03}La_{0.34}Ce_{0.57}Pr_{0.04}Nd_{0.20}Sm_{0.02}Gd_{0.01})_{9.89}(P_{5.78}Si_{0.32})_{6.10}O_{24}F_{2.16}$.

Oka-B. Sample 2 from the Gehlenite Sovite, Bond Zone of the Oka carbonatite (Mariano, 1985). Modal analysis shows a host rock composition of calcite (75%), gehlenite (10%), apatite (4%), phlogopite (3%), magnetite (2%), pyrrhotite (2%), and salite, latrappite, pyrochlore, vesuvianite, and wollastonite (all <1%). The major REE carriers of the Oka-B sovite are apatite, lattrapite, pyrochlore, and calcite. All of these minerals in the Bond Zone rocks show strong LREE preference (Eby, 1975), consistent with primary mineralization in carbonatite magmas. Chemical analysis of the apatite yielded $(Ca_{9.28}Na_{0.04}Sr_{0.10}La_{0.26}Ce_{0.44}Nd_{0.12}Sm_{0.01}Gd_{0.01})_{10.26}(P_{4.89}Si_{0.81}S_{0.04})_{5.74}O_{24}F_{0.67}(OH)_{1.33}$, OH by difference.

Kipawa. Sample 3-K-6 from the Kipawa nepheline syenite complex, Quebec, a metamorphosed agpaitic syenite occurrence as indicated by gneissic texture, deformation, and the development of phlogopite-britholite-diopside skarns, where diopside contains considerably lower Fe^{2+} than observed in igneous diopside. The bulk REE content of the Kipawa rocks shows strong MREE and Y compositions. The major REE carriers are eudialyte, mosandrite, britholite, hiortdahlite, apatite, and agrellite. Apatite is the only REE mineral in Kipawa rocks that displays a strong LREE preference. In all of the varied alkaline rock units at Kipawa, accessory apatite contains anomalous quantities of REE, and therefore most of the apatite separates in S.G. > 3.3 heavy liquid fractions. Despite locally high PO_4 and REE activity of the Kipawa fluids, monazite has not been found to occur. A Kipawa apatite analysis yielded $(Ca_{9.41}Na_{0.10}Sr_{0.03}Y_{0.07}La_{0.11}Ce_{0.22}Nd_{0.07}Sm_{0.01}Gd_{0.01}Dy_{0.01}Er_{0.01})_{10.05}(P_{5.51}Si_{0.44}Ti_{0.01}Al_{0.01})_{5.97}O_{24}F_{1.98}$.

Oka. Roeder et al. (1987) describe the Oka material as primary colorless prisms associated with calcite, salite, phlogopite, and magnetite. The apatite occurs in an apatite sovite near the Britholite Zone of the Oka carbonatite. The analysis yields $(Ca_{9.78}Na_{0.02}Sr_{0.09}Fe_{0.01}Mn_{0.01}Y_{0.01}La_{0.06}Ce_{0.10}Nd_{0.03})_{10.11}(P_{5.55}Si_{0.32})_{5.87}O_{24}F_{1.48}(OH)_{0.52}$, OH by difference.